2007

Infrared spectra of the Li +_(H 2)n(n=1-3) cation complexes

C Emmeluth
University Of Melbourne

B L. J Poad
University of Wollongong, bpoad@uow.edu.au

C D. Thompson
University Of Melbourne

G H. Weddle
University Of Melbourne

E J. Bieske
University Of Melbourne

Recommended Citation

Infrared spectra of the Li +_(H 2)n(n=1-3) cation complexes

Abstract

The $Li^+-(H_2)_n$ n = 1−3 complexes are investigated through infrared spectra recorded in the H−H stretch region (3980−4120 cm^{-1}) and through *ab initio* calculations at the MP2/aug-cc-pVQZ level. The rotationally resolved H−H stretch band of Li^+-H_2 is centered at 4053.4 cm^{-1} [a −108 cm^{-1} shift from the $Q_1(0)$ transition of H_2]. The spectrum exhibits rotational substructure consistent with the complex possessing a T-shaped equilibrium geometry, with the Li^+ ion attached to a slightly perturbed H_2 molecule. Around 100 rovibrational transitions belonging to parallel K_a = 0-0, 1-1, 2-2, and 3-3 subbands are observed. The K_a = 0-0 and 1-1 transitions are fitted by a Watson *A*-reduced Hamiltonian yielding effective molecular parameters. The vibrationally averaged intermolecular separation in the ground vibrational state is estimated as 2.056 Å increasing by 0.004 Å when the H_2 subunit is vibrationally excited. The spectroscopic data are compared to results from rovibrational calculations using recent three dimensional Li^+-H_2 potential energy surfaces [Martinazzo et al., J. Chem. Phys. 119, 11241 (2003); Kraemer and Špirko, Chem. Phys. 330, 190 (2006)]. The H−H stretch band of $Li^+-(H_2)_2$, which is centered at 4055.5 cm^{-1} also exhibits resolved rovibrational structure. The spectroscopic data along with *ab initio* calculations support a $H_2-Li^+-H_2$ geometry, in which the two H_2 molecules are disposed on opposite sides of the central Li^+ ion. The two equivalent $Li^+\cdots H_2$ bonds have approximately the same length as the intermolecular bond in Li^+-H_2. The $Li^+-(H_2)_3$ cluster is predicted to possess a trigonal structure in which a central Li^+ ion is surrounded by three equivalent H_2 molecules. Its infrared spectrum features a broad unresolved band centered at 4060 cm^{-1}.

Keywords
infrared, spectra, cation, li, complexes, h, 2, n, 1, 3, _

Disciplines
Life Sciences | Physical Sciences and Mathematics | Social and Behavioral Sciences

Publication Details

Infrared spectra of the Li+−(H2)_n (n=1−3) cation complexes

C. Emmeluth, B. L. J. Poad, C. D. Thompson, G. H. Weddle,[a] and E. J. Bieske[b]

School of Chemistry, University of Melbourne, Melbourne 3010, Australia

The $Li^+-(H_2)_n$ $n=1-3$ complexes are investigated through infrared spectra recorded in the H–H stretch region (3980–4120 cm^{-1}) and through *ab initio* calculations at the MP2/aug-cc-pVQZ level. The rotationally resolved H–H stretch band of Li^+-H_2 is centered at 4053.4 cm^{-1} [a −108 cm^{-1} shift from the $Q_1(0)$ transition of H_2]. The spectrum exhibits rotational substructure consistent with the complex possessing a T-shaped equilibrium geometry, with the Li^+ ion attached to a slightly perturbed H_2 molecule. Around 100 rovibrational transitions belonging to parallel K_a=0-0, 1-1, 2-2, and 3-3 subbands are observed. The K_a=0-0 and 1-1 transitions are fitted by a Watson A-reduced Hamiltonian yielding effective molecular parameters. The vibrationally averaged intermolecular separation in the ground vibrational state is estimated as 2.056 Å increasing by 0.004 Å when the H_2 subunit is vibrationally excited. The spectroscopic data are compared to results from rovibrational calculations using recent three dimensional Li^+-H_2 potential energy surfaces [Martinazzo *et al.*, J. Chem. Phys. **119**, 11241 (2003); Kraemer and Špirko, Chem. Phys. **330**, 190 (2006)]. The H–H stretch band of $Li^+-(H_2)_2$, which is centered at 4055.5 cm^{-1} also exhibits resolved rovibrational structure. The spectroscopic data along with *ab initio* calculations support a $H_2-Li^+-H_2$ geometry, in which the two H_2 molecules are disposed on opposite sides of the central Li^+ ion. The two equivalent $Li^+\cdots H_2$ bonds have approximately the same length as the intermolecular bond in Li^+-H_2. The $Li^+-(H_2)_3$ cluster is predicted to possess a trigonal structure in which a central Li^+ ion is surrounded by three equivalent H_2 molecules. Its infrared spectrum features a broad unresolved band centered at 4060 cm^{-1}. © *2007 American Institute of Physics.*
[DOI: 10.1063/1.2738464]

I. INTRODUCTION

The Li^+-H_2 complex is one of the simplest charged polyatomic molecules and therefore constitutes a useful benchmark system for assessing computational strategies aimed at describing ion-neutral complexes. More specifically, Li^+-H_2 is relevant to understanding hydrogen storage in zeolites, in which H_2 molecules are attached to alkali metal cation sites,[1] and may also be important in understanding the chemistry of the early universe.[2]

Clampitt and Jefferies made the first observation of $Li^+-(H_2)_n$ clusters by irradiating a solid H_2 target with a Li^+ ion beam.[3] The Li^+-H_2 binding energy was subsequently estimated as 6.5 kcal mol^{-1} (2275 cm^{-1}) through appearance potential measurements in a lithium hydrogen vapor.[4] Most recently, our group obtained a rotationally resolved infrared spectrum of Li^+-D_2 by monitoring Li^+ photofragments as the infrared wavelength was scanned over the D–D stretch band.[5] Analysis of the spectrum confirmed that Li^+-D_2 possesses a T-shaped C_{2v} equilibrium structure, a geometry favored by the electrostatic interaction between the positively charged Li^+ and the D_2 quadrupole moment. Other relevant experimental studies include investigations by Toennies and co-workers of vibrationally and rotationally inelastic collisions between Li^+ and the H_2 and D_2 molecules.[6–9]

A long series of theoretical investigations extending over 40 years has focused on calculating the equilibrium geometry and harmonic vibrational frequencies of Li^+-H_2 and its isotopomers at increasingly sophisticated levels of *ab initio* theory.[10–34] Recently, several groups have acknowledged the likely importance of large amplitude vibrational motions in the spectroscopy and dynamics of the complex and have predicted molecular properties using *ab initio* potential energy surfaces (PESs) and variational rovibrational calculations. A first step in this direction was taken by Searles and von Nagy-Felsobuki who fitted a 170 *ab initio* energy points for Li^+-H_2 with a Padé-approximant function with a Dunham expansion variable.[23] Røcggen *et al.* calculated a $Li^+\cdots H_2$ interaction PES for fixed H_2 bond length that was used in scattering calculations to model the mobility of Li^+ ions in gaseous H_2.[33] Bulychev *et al.* calculated a three-dimensional (3D) PES at the MP2 level and determined the energies for the $J=0$ vibrational states of Li^+-H_2, Li^+-D_2, and Li^+-T_2.[34] Martinazzo-Tantardini-Bodo-Gianturco (MTBG) calculated a 3D PES of the Li^+-H_2 system, primarily to understand the astrophysically important $LiH^++H \rightarrow Li^++H_2$ and $LiH+H^+ \rightarrow Li+H_2^+$ reactions.[2] The MTBG PES was subsequently used in variational calculations to determine the $J=0$ rovibrational states of Li^+-H_2.[35] Recently, Kraemer and Špirko (KS) calculated a new PES that was used to determine the energies of $J=0-5$ bound levels and $J=0$ quasibound states.[36] The KS PES features a somewhat longer equilibrium distance and shallower well than the MTBG PES (1.9870 vs

1.9156 Å for the intermolecular separation and 2156.6 vs 2306.7 cm^{-1} for D_e). Generally, for Li$^+$–D$_2$ there is better correspondence between the experimental data and calculated data for the KS PES than for the MTBG PES. For example, whereas the KS PES slightly underestimates the experimental $\bar{B}$ rotational constant (by 0.7%), the MTBG PES considerably overestimates the $\bar{B}$ rotational constant (by ~5%).

The rotationally resolved Li$^+$–H$_2$ infrared spectrum in the H–H stretch region reported here provides further information for assessing Li$^+$–H$_2$ PESs. The spectroscopic data are compared with results for $J=0-5$ rovibrational calculations reported by Kraemer and Špirko[36] and $J=0-4$ rovibrational calculations using the MTBG PES (energies for the MTBG $J=0$ levels were previously reported by Sanz *et al.*[35]).

As part of the current work, the larger Li$^+$–(H$_2$)$_2$ and Li$^+$–(H$_2$)$_3$ clusters are characterized through their infrared spectra. Although larger Li$^+$–(H$_2$)$_n$ ($n=1-6$) clusters have previously been created by Li$^+$ ion bombardment of solid H$_2$[3] and investigated theoretically,[24,28,31] this, as far as we are aware, is the first report of their IR spectra. *Ab initio* calculations predict that the Li$^+$ ion can bind six H$_2$ molecules in the first solvation shell, and that at least for the smaller clusters, the Li$^+$···H$_2$ bonds are of comparable strength to the intermolecular bond in the Li$^+$–H$_2$ dimer. Significantly, the Li$^+$–(H$_2$)$_2$ spectrum exhibits rotationally resolved features and is analyzed to provide quantitative structural information.

II. EXPERIMENTAL METHODS

Infrared spectra of ^{7}Li$^+$–(H$_2$)$_n$ ($n=1-3$) complexes were obtained in the H–H stretch vibrational region (3990–4110 cm^{-1}) by monitoring ^{7}Li$^+$–(H$_2$)$_{n-1}$ fragments while scanning the IR wavelength. The complexes were produced in a supersonic expansion of H$_2$ (8 bars) passed over a translating and rotating metal rod (10% Li/90% Al) irradiated with the fundamental (1064 nm, 7 mJ/pulse), doubled (532 nm, 3 mJ/pulse), and quadrupled (266 nm, 1 mJ/pulse) 20 Hz output of a pulsed Nd:YAG (yttrium aluminum garnet) laser. The desired ion clusters were selected by a quadrupole mass filter and deflected through 90° by a quadrupole bender into an octopole ion guide, where they were overlapped by the counterpropagating output of a tunable IR source (Continuum Mirage 3000, linewidth of 0.017 cm^{-1}). The resulting photofragments were selected by a second quadrupole mass filter and detected using a microchannel plate coupled to a scintillator and a photomultiplier tube.

The wavelength of the IR light was determined by measuring the wavelengths of the signal output from the first stage of the optical parametric oscillator (OPO) and the 532 nm pump beam of the seeded Nd:YAG laser using a wavemeter (HighFinesse WS/7). Transition wave numbers were corrected to account for the Doppler shift, resulting from the ions' 10 eV translational energy in the octopole ion guide. The absolute uncertainty of the line wave numbers is decided by the uncertainty of the ions' energy in the octopole io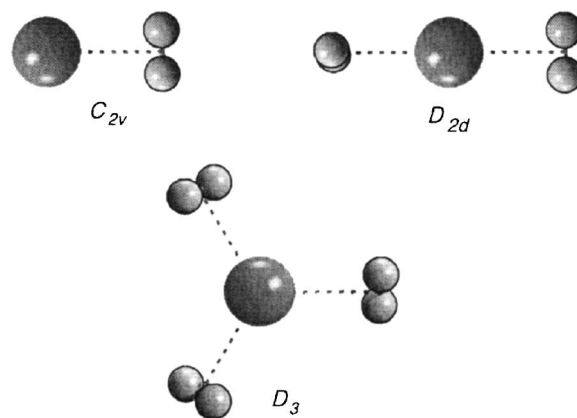n guide and is estimated as ±0.10 cm^{-1}. The relative uncertainty of the lines' wave numbers is estimated as ±0.01 cm^{-1}. Line intensities are not normalized for laser power or parent ion signal intensity (which both exhibit considerable shot-to-shot and longer term fluctuations). Further details of the experimental apparatus can be found in Refs. 5 and 37.

FIG. 1. Minimum energy structures for Li$^+$–(H$_2$)$_n$ $n=1-3$ clusters calculated at the MP2/aug-cc-pVQZ level.

III. RESULTS AND DISCUSSION

A. *Ab initio* calculations

Equilibrium structures, vibrational frequencies, and intensities for the Li$^+$–(H$_2$)$_n$ ($n=1-3$) clusters were calculated at the MP2/aug-cc-pVQZ level. Optimized structures, which are similar to those found in previous studies,[28,31,32] are shown in Fig. 1. The $n=1$ complex has a T-shaped structure (C_{2v} symmetry) with an intermolecular separation of 2.010 Å. The Li$^+$–(H$_2$)$_2$ complex has D_{2d} symmetry with the two H$_2$ subunits positioned on opposite sides of the Li$^+$ and aligned perpendicular to one other (Fig. 1). The two intermolecular bonds have lengths of 2.019 Å. The Li$^+$–(H$_2$)$_3$ cluster has D_3 symmetry; the center of mass of each H$_2$ subunit is disposed about the Li$^+$ cation in a trigonal planar configuration with the H–H bonds tilted out of plane by 44° (Fig. 1). The three intermolecular bonds have lengths of 2.025 Å.

Addition of the second and third H$_2$ molecules leads to a progressive weakening of the Li$^+$···H$_2$ bonds, as evidenced by the 0.009 and 0.006 Å increases in the intermolecular bond length. The slight increase in the intermolecular bond length is consistent with the trend in the calculated H$_2$ stretching vibrational frequencies [$n=1$: 4393 cm^{-1}, int =43.9 km/mol; $n=2$: 4400 cm^{-1} int=0 km/mol, and 4398 cm^{-1} int=74.7 km/mol; $n=3$: 4402 cm^{-1} int =49.5 km/mol (doubly degenerate), 4407 cm^{-1} int =0 km/mol]. For reference, the H$_2$ molecule was calculated to have a harmonic frequency of 4515 cm^{-1}. Scaling the cluster H–H stretch frequencies by the factor required to reconcile the calculated and experimental frequencies for the free H$_2$ molecule (0.9216) gives frequencies of 4049, 4053, and 4057 cm^{-1} for the IR active H–H stretch vibrations of the $n=1-3$ clusters, respectively.
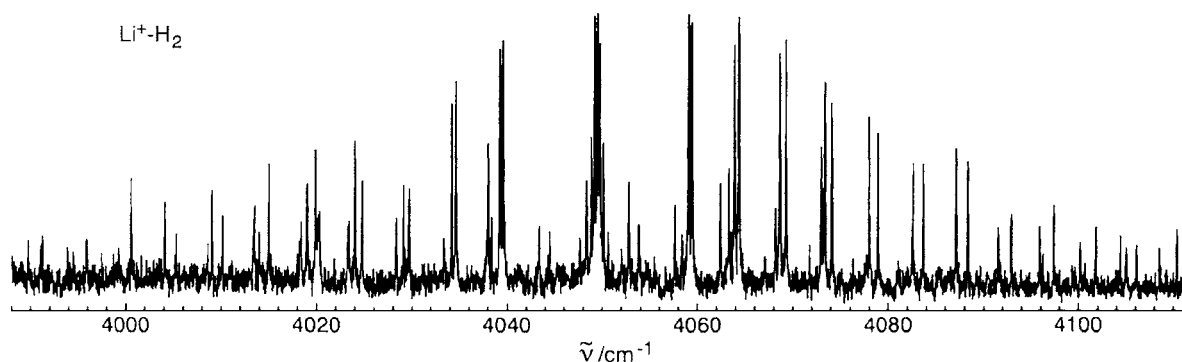
FIG. 2. Infrared spectrum of ^{7}Li$^+$–H$_2$ in the H–H stretch region recorded by monitoring Li$^+$ photofragments. The central feature is the K_a=1-1 Q branch. Line wave numbers are available as supplementary material (Ref. 41).

B. Li$^+$–H$_2$

1. Infrared spectrum

The calculated equilibrium structure of Li$^+$–H$_2$ shown in Fig. 1 is associated with rotational constants of A =60.26 cm^{-1}, B=2.66 cm^{-1}, and C=2.55 cm^{-1}, and is near the prolate symmetric rotor limit (asymmetry parameter κ=−0.996). Therefore K_a should be a nearly good quantum number. Furthermore, internal rotation of the H$_2$ subunit should be mostly quenched since the rotational constant for H$_2$ ($b_{HH} \sim 60$ cm^{-1}) is considerably less than the barrier to internal rotation (1680 cm^{-1}; Ref. 2). Because the transition moment associated with vibrational excitation of the H$_2$ sub-unit lies along the intermolecular bond, one expects an A-type band consisting of overlapping K_a=0-0, 1-1, 2-2, etc. subbands.

The IR spectrum of the Li$^+$–H$_2$ complex in the H–H stretch region (shown in Fig. 2) conforms with the expectations outlined above. Approximately 100 lines have been measured and assigned. Of these lines, 19 are assigned to K_a=0-0 transitions, 50 to K_a=1-1 transitions (P branch: 20 lines, Q branch: 8 lines, R branch: 22 lines), 17 to K_a=2-2 transitions, and 13 to K_a=3-3 transitions. The central region of the spectrum (enlarged in Fig. 3) displays conspicuous Q branches for the K_a=1-1, 2-2, and 3-3 subbands, although
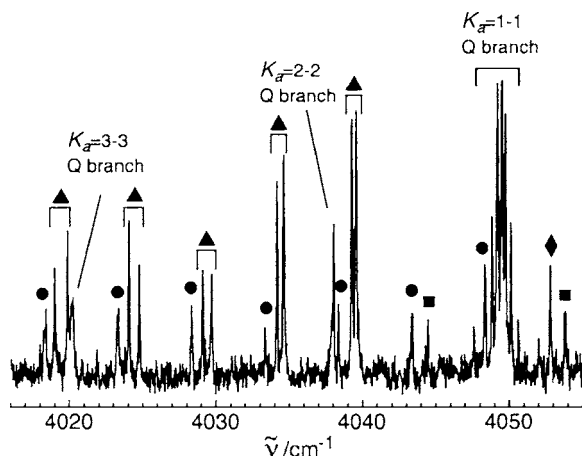

FIG. 3. Expanded view of the central part of the Li$^+$–H$_2$ IR spectrum shown in Fig. 2. The K_a=0-0 transitions are indicated by filled circles (●), the K_a=1-1 transitions by triangles (▲), the K_a=2-2 transitions by diamonds (♦), and the K_a=3-3 transitions by squares (■).

individual transitions are only resolved for the K_a=1-1 sub-band. Similarly, asymmetry splittings are resolved in the P and R branches of the K_a=1-1 subband but are not distin-guishable in the K_a=2-2 and K_a=3-3 subbands, for which the splitting is anticipated to be much smaller. In terms of its overall structure, the spectrum is very similar to that of Li$^+$–D$_2$.[5]

For the ground vibrational state, even and odd K_a levels correspond to Li$^+$–H$_2$ complexes containing, respectively, *para* (even j) and *ortho* (odd j) modifications of H$_2$. For normal H$_2$ gas the *para* and *ortho* forms occur in a 1:3 ratio. The observed intensity ratio for the even to odd K_a lines is approximately 1:5 rather than 1:3. The predominance of complexes containing *ortho* hydrogen over those containing *para* hydrogen has been noted for a range of neutral and charged species.[38,39] The explanation is that *ortho* H$_2$ is easier to orient in an electric field than *para* H$_2$ so that the Li$^+\cdots$H$_2$(o) bond is stronger than the Li$^+\cdots$H$_2$(p) bond. Di-rect collisional relaxation between the two forms should be extremely inefficient in the supersonic expansion, although exchange of H$_2$ ligands attached to the Li$^+$ probably occurs in the early part of the supersonic expansion.

2. Asymmetric rotor analysis

The wave numbers for the K_a=0-0 and 1-1 lines were fitted using an A-reduced Watson Hamiltonian. Adjustable parameters included the B and C rotational constants and Δ_J, Δ_{JK}, and δ_J centrifugal distortion terms. Note that for Li$^+$–D$_2$ it was not necessary to include the δ_J term to fit adequately the K_a=0-0 and K_a=1-1 lines. Although inclu-sion of the additional quartic centrifugal distortion term Δ_K enabled the K_a=2-2 transitions to be fitted together with the K_a=0-0 and K_a=1-1 transitions (albeit with a marked in-crease in rms error), extending the data set to include the K_a=3-3 lines resulted in a very poor fit. The difficulty in fitting the transitions with a reasonable number of adjustable parameters is presumably a consequence of the large ampli-tude zero-point motions in the bending/hindered rotation and intermolecular stretch coordinates. It is not possible through analysis of the A-type transition to determine A'' or A' di-rectly; rather, $\Delta A = A' - A''$ is ascertained. For the purpose of the fit, A'' was constrained to 59.34 cm^{-1}, the ground state rotational constant for free H$_2$.[40] Resulting parameters are listed in Table I, which also includes parameters for separate

TABLE I. Constants in cm^{-1} for Li^+–H_2 obtained by fitting the H–H stretch band K_a=0-0 and 1-1 transitions to a Watson A-reduced Hamiltonian. Also listed are constants obtained by fitting separately the K_a=0-0, 1-1, and 2-2 transitions. The error in the last significant figure(s) is given in brackets.

	$K_a=0$	$K_a=1$	$K_a=2$	$K_a=0,1$
B''	$\cdots$	2.5645(9)	$\cdots$	2.5700(9)
C''	$\cdots$	2.4128(9)	$\cdots$	2.4183(9)
$\bar{B}''$	2.4941(4)	2.4887(9)	2.4766(27)	2.4942(9)
$\Delta_J'' \times 10^4$	3.29(2)	3.18(3)	4.1(7)	3.18(3)
$\Delta_{JK}'' \times 10^3$	$\cdots$	$\cdots$	$\cdots$	5.5(4)
$\delta_J'' \times 10^5$	$\cdots$	1.7(2)	$\cdots$	1.7(2)
B'	$\cdots$	2.5530(9)	$\cdots$	2.5580(9)
C'	$\cdots$	2.4003(8)	$\cdots$	2.4052(8)
$\bar{B}'$	2.4819(4)	2.4767(9)	2.4646(20)	2.4816(9)
$\Delta_J' \times 10^4$	3.20(2)	3.06(3)	3.4(4)	3.06(3)
$\Delta_{JK}' \times 10^3$	$\cdots$	$\cdots$	$\cdots$	5.0(4)
$\delta_J' \times 10^5$	$\cdots$	1.46(21)	$\cdots$	1.5(2)
ΔA	$\cdots$	$\cdots$	$\cdots$	4.022(9)
ν_0	4053.360(4)	4049.340(12)	4038.039(43)	4053.367(8)
rms$\times 10^3$	1.4	6.2	8.9	6.0

fits to the K_a=0-0, K_a=1-1, and K_a=2-2 subbands. Line wave numbers, assignments, and differences between fitted and measured wave numbers are provided as supplementary material.[41]

Generally, the spectroscopic constants are compatible with expectations based on previous *ab initio* calculations and the Li^+–D_2 spectroscopic results. For example, the ground and excited state vibrationally averaged $Li^+\cdots H_2$ separations estimated from $\bar{B}''$ and $\bar{B}'$ are 2.056 and 2.060 Å, respectively, comparable with equilibrium separations determined in recent *ab initio* calculations (e.g., 2.010 Å from the MP2/aug-cc-pVQZ calculations described in Sec. III A and Ref. 32), and also with the corresponding Li^+–D_2 spectroscopic results (2.036 and 2.039 Å, respectively).

Consideration of the spectroscopic data in Table I suggests that even in the ground vibrational state, Li^+–H_2 undergoes large amplitude vibrational excursions, particularly

in the bending/hindered internal rotation coordinate. A rigid planar molecule should have an inertial defect $\Delta = 1/C - 1/B - 1/A$ of zero. Taking the experimental values for B'' and C'' (Table I) into account one finds $A'' = 40.8$ cm^{-1}, corresponding to a vibrationally averaged H–H separation of 0.90 Å. This represents a large increase (by 0.15 Å) in the H–H bond length compared to the free H_2 molecule value ($\langle\langle r \rangle\rangle = 0.75$ Å) that is unlikely to be caused by the relatively weak interaction with the Li^+ ion. For the Li^+–D_2 complex, a similarly unlikely though different D–D bond length (0.83 Å) was deduced on the basis of the B and C rotational constants and assumption of zero intertial defect.[5] A more probable alternative to large distortions of the H_2 and D_2 subunits is that the effective molecular parameters (B and C) are influenced by the large amplitude bending/hindered rotations in the complexes. As pointed out by Lovejoy *et al.*[38] and Nesbitt and Naaman,[42] the unquenched hindered internal rotation in T-shaped complexes tends to exaggerate the asymmetry doubling and consequently B-C, leading to a nonzero inertial defect. The effect becomes larger as the hindering barrier decreases.

3. Comparison with calculated energy levels

One goal of this work is to evaluate the MTBG and KS *ab initio* PESs for Li^+–H_2 through comparisons of the spectroscopic data and theoretical predictions. Using their PES, Kraemer and Špirko[36] calculated and reported energies for the $J=0-5$ levels of Li^+–H_2, allowing relatively direct links to be made with the spectroscopic data. For the MTBG PES only energies for the $J=0$ levels have been reported previously,[35] to enable comparisons with the experimental data we have undertaken rovibrational calculations for the $J=0-4$ levels. The calculations, which were performed using the TRIATOM program,[43] utilized a basis set comprising 7 Morse functions in the H–H stretch, 24 Morse functions in the intermolecular stretch, and 15 Legendre functions for the angular coordinate. The masses of the Li and H atoms were taken as 7.016 00 and 1.007 825 amu, respectively. Energies

TABLE II. Energies for the lowest $J=0-4$ levels of Li^+–H_2 calculated using the MTBG PES from Ref. 2. Effective rotational constants ($\bar{B}$ and D_J) for each manifold are given at bottom. Calculated values of $\bar{B}$ and D_J obtained using the KS PES from Ref. 36 are given in brackets.

J	$K_a=0$	$K_a=1$	$K_a=2$	$K_a=3$
0	0			
1	5.212	66.996		
		67.156		
2	15.627	77.232	260.447	
		77.711	260.447	
3	31.230	92.567	275.932	575.230
		93.524	275.932	575.230
4	51.997	112.980	296.544	595.651
		114.571	296.545	595.651
$\bar{B}$	2.606(2.477)	2.601(2.469)	2.586(2.459)	2.553
$D_J \times 10^4$	3.27(3.28)	3.17(2.65)	3.08(3.6)	$\cdots$

TABLE III. Experimental and calculated data relating to asymmetry splittings [$\Delta''(J)$ and $\Delta'(J)$] for the $K_a=1$ manifolds. Results determined using the KS PES (Ref. 36) are given in brackets.

J	$\Delta''(J)_{\text{calc}}$	$\bar{\Delta}(J)_{\text{exp}}$ [a]	$\Delta''_1(J)_{\text{calc}}$ [b]	$\Delta''_1(J)_{\text{exp}}$ [b]	$\Delta'_1(J)_{\text{exp}}$ [c]
1	0.160	0.154	0.640	0.611	0.627
2	0.480(0.4)	0.465	1.437(1.3)	1.360	1.357
3	0.957(0.9)	0.893	2.548(2.4)	2.381	2.419
4	1.591(1.5)	1.507	(3.8)	3.759	3.767

[a]$\Delta(J)=\frac{1}{2}(\Delta''(J)+\Delta'(J))$.
[b]$\Delta''_1(J)=\Delta''(J)+\Delta''(J+1)$.
[c]$\Delta'_1(J)=\Delta'(J)+\Delta'(J+1)$.

for the lower $J=0-4$ rovibrational levels, converged to $<10^{-3}$ cm^{-1}, are listed in Table II. In agreement with Ref. 35, it was found that the ground ($v_{\text{HH}}=0$, $v_s=0$, $v_b=0$, $J=0$) state of Li$^+$–H$_2$ lies 1732 cm^{-1} below the Li$^+$+H$_2$ ($v_{\text{HH}}=0$, $j=0$) asymptote.

To facilitate comparisons with the experimental data, energies for the $K_a=0$, 1, and 2 manifolds were fitted independently to a polynomial in $J(J+1)$ to give effective $\bar{B}$ and D_J values. Results from these fits are also given in Table II. For the $K_a=0$ manifold, the $\bar{B}$ value derived from the MTBG rovibrational levels (2.606 cm^{-1}) is 4.5% greater than the experimental value (2.494 cm^{-1}), suggesting that the intermolecular separation is underestimated. In comparison, the $\bar{B}$ value associated with the KS $K_a=0$ rovibrational levels (2.477 cm^{-1}) is slightly less (by 0.007%) than the experimental value indicating that the intermolecular separation is overestimated slightly.[36] The differences between the MTBG, KS, and experimental $\bar{B}$ values for the $K_a=1$ and 2 manifolds follow a similar trend to the $K_a=0$ results.

The $K_a=1$ asymmetry splittings are sensitive to details of the Li$^+$⋯H$_2$ PES, increasing as the hindering barrier for H$_2$ internal rotation decreases and as the intermolecular bond shortens. For this reason it would be interesting to compare experimental and calculated $K_a=1$ asymmetry splittings. While the lower and upper state splittings $\Delta''(J)$ and $\Delta'(J)$ cannot be determined directly from the infrared spectrum, using combination differences, one can ascertain $\Delta''_1(J)=\Delta''(J)+\Delta''(J+1)$, $\Delta'_1(J)=\Delta'(J)+\Delta'(J+1)$ and $\bar{\Delta}(J)=\frac{1}{2}(\Delta''(J)+\Delta'(J))$. The experimental and calculated data are compiled in Table III.

In considering the asymmetry splittings two points are worth noting. First, because the experimental $\Delta''_1(J)$ and $\Delta'_1(J)$ values are very similar, it appears that vibrational excitation of the H$_2$ subunit has little effect on the molecular geometry or the barrier for hindered internal rotation. This accords with the relatively minor differences between ground and excited state rotational constants derived from the semirigid rotor analysis (Table I). Second, it seems that the experimental $K_a=1$ asymmetry splittings are overestimated by calculations using the MTBG PES ($\Delta''_1(J)_{\text{calc}}>\Delta''_1(J)_{\text{expt}}$). This suggests that the MTBG PES underestimates the barrier to hindered internal rotation of the H$_2$ subunit and/or the intermolecular separation; from comparisons between the experimental and calculated $\bar{B}$ values the latter is almost certainly the case. Generally, the $\Delta''_1(J)_{\text{calc}}$ values derived using

the KS PES appear to be closer to the experimental values, although detailed comparisons are difficult because the relevant rovibrational energies in Ref. 36 are only reported to a single decimal place.

Conclusions presented here concerning the adequacy of the MTBG PES for representing the Li$^+$–H$_2$ interaction are consistent with our previous study of Li$^+$–D$_2$, where it was also found that the PES underestimated somewhat the Li$^+$⋯D$_2$ separation.[5] Generally, both the Li$^+$–H$_2$ and Li$^+$–D$_2$ complexes appear to be described better by the KS PES. However, when judging the MTGB PES it should be remembered that it is a global surface, describing not only the weakly bound Li$^+$–H$_2$ complex but also the LiH$^+$+H →Li$^+$+H$_2$ and LiH+H$^+$→Li+H$_2^+$ reactions.[2]

4. Intermolecular vibrational modes

The harmonic intermolecular stretch frequency can be estimated from the experimental spectroscopic constants (B and D_J); approximating the complex as a pseudodiatomic, one finds $\omega''_s \simeq \omega'_s \simeq 440$ cm^{-1}. This value is consistent with calculated v_s values found using the MTBG PES (426.20 cm^{-1}; Ref. 35), using the KS PES (405.1 cm^{-1}; Ref. 36), and by Bulychev et al. (399.0 cm^{-1}; Ref. 34). The experimental spectrum does not provide direct information on the intermolecular bending frequency v_b, which has been calculated as 646.61 cm^{-1} (MTBG PES; Ref. 35), 594.2 cm^{-1} (KS PES; Ref. 36), and 588.5 cm^{-1} (by Bulychev et al.; Ref. 34). Spectroscopic observation of the $v_{\text{HH}}+v_s$ and $v_{\text{HH}}+v_b$ combination bands would provide more direct experimental information on the intermolecular modes that could be compared with calculated data and further test the PESs.

5. Ground/excited state changes and vibrational redshift

The band center of the Li$^+$–H$_2$ $v_{\text{HH}}=1 \leftarrow v_{\text{HH}}=0$ transition occurs at 4053.4 cm^{-1}, representing a redshift of 107.8 cm^{-1} with respect to the $Q_1(0)$ transition of the free H$_2$ molecule (4161.2 cm^{-1}; Ref. 44). The measured redshift is close to values calculated by Bulychev et al. (105.4 cm^{-1}; Ref. 34), Bishop and Cybulski (110.7 cm^{-1}; Ref. 26), and the scaled MP2/aug-cc-pVQZ result (112 cm^{-1}; Sec. III A and Ref. 32). Furthermore, the relative redshifts $\Delta\nu/\nu$ for Li$^+$–H$_2$ and Li$^+$–D$_2$ are very similar (2.6% in both cases) and are comparable to other cation-dihydrogen complexes [e.g., $\Delta\nu/\nu=2.8\%$ for H$_2$–H$_3$O$^+$ (Ref. 45) and 2.3% for H$_2$–HCO$^+$ (Ref. 46)].

The redshift can be interpreted as the difference between the intermolecular binding energies of Li$^+$ interacting with H$_2$ in the $v_{\text{HH}}=0$ and $v_{\text{HH}}=1$ states. From this perspective the effective Li$^+$⋯H$_2(v_{\text{HH}}=1)$ potential surface is deeper than the Li$^+$⋯H$_2(v_{\text{HH}}=0)$ potential surface by 107.8 cm^{-1}. The stronger excited state interaction is consistent with increases in the quadrupole moment and polarizability of H$_2$ by around 10% for the $v_{\text{HH}}=1$ state compared to the $v_{\text{HH}}=0$ state,[47] leading to enhancements of the charge-quadrupole interaction and charge induced dipole induction interaction.

Notwithstanding the 107.8 cm^{-1} increase in the effective Li$^+\cdots$H$_2$ interaction energy, the A, B, and C rotational constants derived from the semirigid rotor analysis decrease when the H$_2$ subunit is vibrationally excited, suggesting that there is a slight increase in the vibrationally averaged intermolecular separations. A similar phenomenon was noted in our earlier study of Li$^+$–D$_2$.[5] The 4.02 cm^{-1} decrease in A is expected because the rotational constant of the free H$_2$ molecule diminishes by 3.97 cm^{-1} going from $v_{HH}=0$ to $v_{HH}=1$.[40] Reductions in the B and C constants are more surprising. We note that Bulychev *et al.* found a similar effect, predicting that the vibrationally averaged intermolecular separation increased by 0.006 Å when the H–H stretch is excited.[34] The form of the MTBG surface is also consistent with the slight increase in the intermolecular separation as the equilibrium intermolecular separation increases with the length of the H–H bond, so that averaging over the H–H vibrational stretch wave function leads to a larger mean intermolecular separation for the $v_{HH}=1$ state than for the $v_{HH}=0$ state.[2]

6. Vibrational predissociation dynamics

The $v_{HH}=1 \leftarrow v_{HH}=0$ transitions access quasibound levels that are coupled to the Li$^+$+H$_2(v_{HH}=0)$ continuum. In principle, information on the vibrational predissociation rate can be extracted from the widths of the individual rovibrational lines. Several of the more intense $K_a=1$-1 lines were used to estimate the contribution due to lifetime broadening by fitting them to a Voigt profile with the full width half maximum of the Gaussian component fixed to 0.017 cm^{-1} (the bandwidth of the OPO *IR* radiation). The width of the resulting Lorentzian component is 0.09 ± 0.02 cm^{-1}, corresponding to an upper state lifetime of $\tau_{vp}=60$ ps, somewhat shorter than the value for Li$^+$–D$_2$ ($\tau_{vp}=150$ ps).[5] We caution that these τ_{vp} values should be taken as a lower limits as the lines may be power broadened or Doppler broadened due to the ions having a spread of energy in the octopole region where they overlap with *IR* radiation. It should be noted, however, that using the same instrument we have observed narrower, laser-limited transitions for Br$^-$–D$_2$ and I$^-$–D$_2$.[48,49] Nevertheless, the measured Li$^+$–H$_2$ linewidths are comparable with the prediction of Sanz *et al.*, who calculated lifetimes in the 100–400 ps range for quasibound $v_{HH}=1$ levels,[35] and with the predictions of Kraemer and Špirko who calculated a lifetime of 220 ps for the $v_{HH}=1$, $K_a=0$, $J=0$ level.[36]

C. Li$^+$–(H$_2$)$_2$

The MP2/aug-cc-pVQZ calculations predict that Li$^+$–(H$_2$)$_2$ in its equilibrium configuration has D_{2d} symmetry with the two H$_2$ subunits aligned perpendicular to one other (Figs. 1 and 4). This configuration corresponds to a prolate top (rotational constants $A=30.16$ cm^{-1} and $B=C=1.01$ cm^{-1}), possessing symmetric (a_1), and asymmetric (b_2) H–H stretch vibrations, although only the latter is infrared active (predicted intensity of 74.7 km/mol). Obviously, the Li$^+$–(H$_2$)$_2$ complex is a highly fluxional system in the torsional, bending, and intermolecular stretch coordinates. In
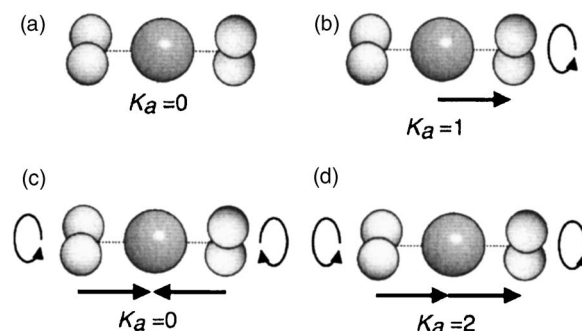

FIG. 4. Low energy forms of Li$^+$–(H$_2$)$_2$ containing (a) two *para* H$_2$ molecules ($K_a=0$), (b) one *para* and one *ortho* H$_2$ molecule ($K_a=1$), (c) two *ortho* H$_2$ molecules ($K_a=0$), and (d) two *ortho* H$_2$ molecules ($K_a=2$).

particular, the barrier for torsional motion is expected to be very low; at the MP2/aug-cc-pVQZ level the staggered configuration is predicted to lie only 2.5 cm^{-1} lower in energy than the eclipsed configuration.

Presumably, the experimentally probed Li$^+$–(H$_2$)$_2$ complexes can exist in several essentially noninterconverting forms. For example, as shown in Fig. 4, the complex could contain two *para* H$_2$ molecules ($K_a=0$), one *para* H$_2$ and one *ortho* H$_2$ molecule ($K_a=1$), or two *ortho* H$_2$ molecules ($K_a=0$ or $K_a=2$, depending, respectively, on whether the projection of the two *ortho* H$_2$ molecules' angular momenta onto the molecular axis is antialigned or aligned). Statistically, the relative populations of the (*para,para*), (*para,ortho*), and (*ortho,ortho*) forms should be 1:6:9.

Overall, one can expect that the infrared spectrum will contain five subbands corresponding to the $K_a=0$-0 subband of the (*para,para*) form, two $K_a=1$-1 subbands of the (*para,ortho*) form (distinguished by the vibrational excitation being localized on either the *para* or the *ortho* subunit), and $K_a=0$-0 and $K_a=2$-2 subbands associated with the (*ortho,ortho*) form. Generally, complexes containing *ortho* H$_2$ will tend to be favored because of their greater statistical weight and enhanced stability compared to complexes containing *para* H$_2$. Therefore, one can expect that the $K_a=0$-0 subband associated with the (*para,para*) form will make a minor contribution to the spectrum.

The experimental infrared spectrum of Li$^+$–(H$_2$)$_2$ (shown in Fig. 5) is dominated by a sharp Q branch flanked by several sets of P- and R-branch lines. Wave numbers and assignments of the lines are available as supplementary material.[41] A complete analysis of the spectrum is difficult due to poor S/N and overlapping of lines in some regions. Nevertheless, the spectrum appears to contain at least three subbands. The most obvious subband includes the central Q branch that dominates the spectrum (at 4053.73 cm^{-1}) and a series of P- and R-branch lines, the first of which is, in each case, separated from the Q branch by $\sim$6.3 cm^{-1}. Subsequent P- and R-branch lines in the subband are spaced by 2.1 cm^{-1}. These features are assigned to the $K_a=2$-2 subband of the (*ortho,ortho*) complex having $B''\simeq B'\simeq1.05$ cm^{-1}. The P- and R-branch lines are quite sharp, showing no obvious asymmetry doubling.

Two other series of lines are apparent in the R-branch region, but overlap in the P-branch region. One of these
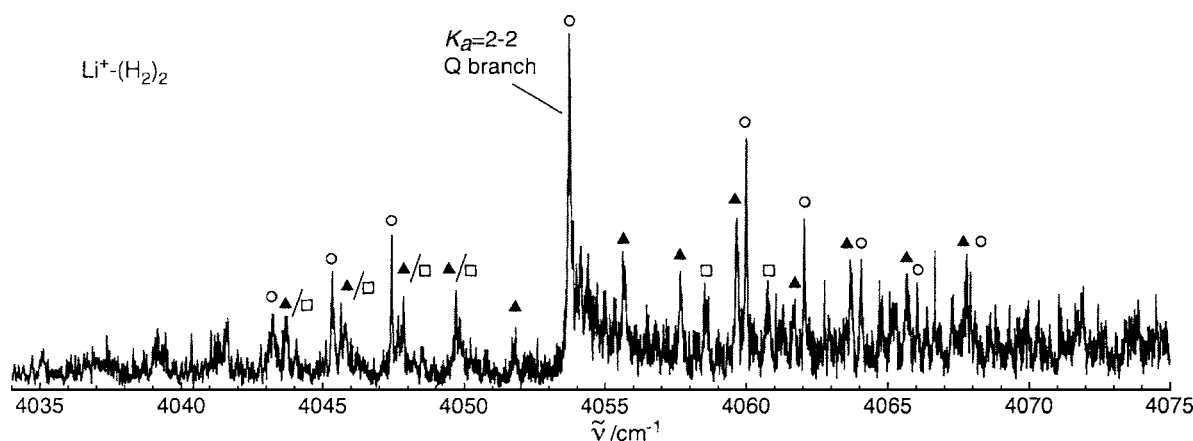
FIG. 5. Infrared spectrum of ^{7}Li$^+$–(H$_2$)$_2$ in the H–H stretch region. The K_a=0-0 transitions are indicated by triangles (▲), K_a=1-1 transitions by open squares (□), and K_a=2-2 transitions by open circles (○).

series appears to be a K_a=0-0 subband, that shares a common origin with the K_a=2-2 subband, and is assigned to the K_a=0 form of the (ortho,ortho) complex. The other series exhibits fewer transitions and is tentatively assigned to one of the K_a=1-1 transitions of the (para,ortho) form. These lines are generally broader than the K_a=2-2 lines, possibly due to unresolved asymmetry doubling. Only two rather broad and noisy R-branch lines are clearly resolved for the K_a=1-1 subband. If the lower frequency line (at 4058.60 cm^{-1}) is assumed to be the $R(1)$ transition, the Q branch of the K_a=1-1 subband can be estimated to occur at ~4054.6 cm^{-1}. This corresponds to a rather broad shoulder on the higher energy side of the K_a=2-2 Q branch.

Constants obtained by fitting separately the K_a=0-0 and K_a=2-2 transitions to a linear molecule transition energy expression are given in Table IV. The origins of the (ortho, ortho) K_a=0-0 and K_a=2-2 subbands are almost the same (4053.7 cm^{-1}), whereas the (para,ortho) K_a=1-1 subband origin lies slightly higher in energy (4054.6 cm^{-1}). Significantly, the Li$^+$–(H$_2$)$_2$ subband origins lie only slightly higher in energy than the origin of the Li$^+$–H$_2$ H–H stretch band (4053.4 cm^{-1}), suggesting that the intermolecular Li$^+$···H$_2$ bonds in Li$^+$–H$_2$ and Li$^+$–(H$_2$)$_2$ are of very similar strength.

Assuming that Li$^+$–(H$_2$)$_2$ has a symmetric linear structure (as suggested by the MP2/aug-cc-pVQZ calculations described in Sec. III A), the vibrationally averaged Li$^+$···H$_2$ separation can be estimated from the B'' constants as R =2.05 Å for the K_a=0 manifold and R=1.98 Å for the K_a =2 manifold. The difference in the effective intermolecular separations for the K_a=0 and 2 manifolds may reflect the

effect of the torsional potential; naively, one might explain the larger intermolecular separation associated with the K_a =0 manifold as reflecting the fact that the H$_2$ molecules are essentially contrarotating, so that they are effectively "knocking against" one another. Although the MP2/aug-cc-pVQZ calculations predict a very small torsional barrier (2.5 cm^{-1}) and minor increase in the intermolecular separation going from the staggered to the eclipsed configuration (0.0003 Å), the actual torsional barrier and bond length change may be larger. For example, the CCSD calculations of Davy et al.[28] predicted a harmonic frequency of 51 cm^{-1} for the torsional vibration, implying a substantially larger barrier than found from the MP2/aug-cc-pVQZ calculations.

Curiously, the average of the separations estimated for the K_a=0 and K_a=2 manifolds (2.01 Å) is slightly less than the vibrationally averaged intermolecular separation for Li$^+$–H$_2$ (2.05 Å). This observation is apparently at odds with the MP2/aug-cc-pVQZ calculations that predict that the Li$^+$–(H$_2$)$_2$ bonds are 0.009 Å longer than the Li$^+$–H$_2$ bond. However, in relating rotational constants to bond distances one should be mindful that Li$^+$–(H$_2$)$_2$ is undoubtedly a very floppy system experiencing large amplitude zero-point excursions, particularly in the intermolecular bending coordinate.

To some extent, the Li$^+$–(H$_2$)$_2$ system probably resembles a molecular "hinge," in which the two H$_2$ molecules are able to move easily about the central Li$^+$. Although the linear H$_2$···Li$^+$···H$_2$ configuration may be the minimum (corresponding to a bond angle θ=0°), bending the system and moving the H$_2$ molecules together should be a facile process (at least until the H$_2$ molecules come into contact near θ=180°). Nesbitt and Naaman have calculated the rovibrational energy levels of a model triatomic system with the bending potential energy curve having a flat-bottomed $V_{\text{hinge}}\theta^6$ dependence, and where the bonds between the two outer atoms and the inner atom are of fixed length.[42] The rotational energy levels were fitted with a Watson asymmetric rotor Hamiltonian to determine effective rotational constants (including A, B, and C). Significantly, as the hinge becomes floppier (V_{hinge} diminishes), the effective B and C rotational constants increase. The situation may be similar for the Li$^+$–(H$_2$)$_2$ system; large amplitude bending motion

TABLE IV. Constants (in cm^{-1}) for the K_a=0-0, 1-1, and 2-2 subbands of Li$^+$–(H$_2$)$_2$. The error in the last significant figure(s) is given in brackets.

	K_a=0-0	K_a=1-1	K_a=2-2
B''	0.982(5)	⋯	1.050(3)
$D_J'' \times 10^4$	⋯	⋯	1.5(7)
B'	0.986(4)	⋯	1.050(2)
$D_J' \times 10^4$	⋯	⋯	2.4(4)
ν_0	4053.72(2)	4054.6[a]	4053.74(4)
rms $\times 10^3$	5	⋯	7

[a]Estimated value, see text.
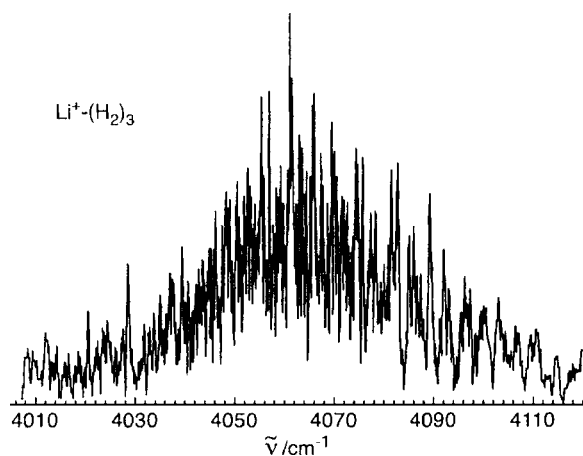
FIG. 6. Infrared spectrum of $Li^+-(H_2)_3$ in the H–H stretch region.

(even in the ground vibrational state) leads to a $\bar{B}$ rotational constant that is larger than for a rigid linear configuration and, which, if interpreted in terms of a rigid linear structure yields an artificially short estimate for the $Li^+\cdots H_2$ bonds.

D. $Li^+-(H_2)_3$

The MP2/aug-cc-pVQZ calculations outlined in Sec. III A predict that $Li^+-(H_2)_3$ possesses a D_3 symmetry structure, with the center of mass for each H_2 subunit disposed about the cation in trigonal planar configuration and with the H–H bonds tilted out of plane (Fig. 1). This structure corresponds to an oblate symmetric top with rotational constants $A=B=1.29$ cm^{-1} and $C=0.67$ cm^{-1}. Obviously, the $Li^+-(H_2)_3$ vibration-rotation-tunneling spectrum will be complicated due to the fact that the complex possesses four different low energy forms containing, respectively, three *para* H_2, two *para* H_2 and one *ortho* H_2, one *para* H_2 and two *ortho* H_2, or three *ortho* H_2 molecules. Each of these forms should exhibit subtly different spectra that will overlap.

The experimental infrared spectrum of $Li^+-(H_2)_3$ (Fig. 6) is congested and noisy, featuring single broad band centered at 4060 ± 5 cm^{-1} with a width of ~35 cm^{-1}. It is unclear whether at higher resolution and with better S/N the $Li^+-(H_2)_3$ spectrum will exhibit resolved rotational transitions or whether these features will be obscured by a combination of spectral congestion and lifetime broadening.

Finally, we note that the experimental frequencies for the H–H stretch bands of the $Li^+-(H_2)_n$ ($n=1-3$) clusters (4053.4, 4055, and 4060 cm^{-1}) correspond quite well with the scaled harmonic frequencies derived from the MP2/aug-cc-pVQZ calculations described in Sec. III A (4049, 4053, and 4057 cm^{-1}). The fact that the H–H vibrational frequencies are very similar confirms that the $Li^+\cdots H_2$ intermolecular bonds in the $n=2$ and 3 clusters are only slightly weaker than the single bond in Li^+-H_2. The calculations of Davy *et al.*[28] and Barbatti *et al.*[31] suggest that the energy required to remove a single H_2 molecule from the clusters declines only slightly for $n=1-4$ with larger drops occurring at $n=5$ and particularly at $n=7$, for which one of the H_2 molecules is situated in the second solvation shell.

IV. SUMMARY

The main conclusions of this work can be summarized as follows.

(1) The Li^+-H_2 complex possesses a rotationally resolved H–H stretch band redshifted by 107.8 cm^{-1} from the stretch fundamental of the bare H_2 molecule.

(2) The Li^+-H_2 complex has a T-shaped equilibrium structure with a vibrationally averaged intermolecular $Li^+\cdots H_2$ separation of ~2.056 Å, increasing by 0.004 Å when the H_2 subunit is vibrationally excited.

(3) A lower 60 ps limit for the predissociation lifetime for $Li^+-H_2(v_{HH}=1)$ is estimated from line broadening.

(4) Generally, it seems that the Li^+-H_2 complex is better described by the KS PES (Ref. 36) than the MTBG PES,[2] which appears to significantly underestimate the intermolecular separation.

(5) The $Li^+-(H_2)_2$ complex is predicted to possess a $H_2-Li^+-H_2$ equilibrium structure with the two H_2 molecules disposed on opposite sides of the central Li^+ ion. The $Li^+-(H_2)_2$ spectrum exhibits a H–H stretch band redshifted by ~106 cm^{-1} from the stretch fundamental of the bare H_2 molecule. The band's rovibrational structure is consistent with a linear or quasi-linear geometry with two equivalent $Li^+\cdots H_2$ bonds each having approximately the same length as the bond in Li^+-H_2.

(6) The $Li^+-(H_2)_3$ complex, which is predicted to possess a trigonal D_3 symmetry equilibrium structure, exhibits a broad unresolved H–H stretch band with a center redshifted by ~100 cm^{-1} from the stretch fundamental of the bare H_2 molecule.

Note added in proof: Since, the submission of this article a paper by Page and von Nagy-Felsobuki has appeared describing a new PES for Li^+-H_2 and accompanying rovibrational calculations for Li^+-H_2, Li^+-HD and Li^+-D_2.[50]

[1] P. Nachtigall, E. Garrone, G. Turnes Palomino, M. Rodríguez Delgado, D. Nachtigallová, and C. Otero Areán, Phys. Chem. Chem. Phys. **8**, 2286 (2006).
[2] R. Martinazzo, G. Tantardini, E. Bodo, and F. Gianturco, J. Chem. Phys. **119**, 11241 (2003).
[3] R. Clampitt and D. K. Jefferies, Nature (London) **226**, 141 (1970).
[4] C. H. Wu, J. Chem. Phys. **71**, 783 (1979).
[5] C. Thompson, C. Emmeluth, B. Poad, G. Weddle, and E. Bieske, J. Chem. Phys. **125**, 044310 (2006).
[6] J. Schottle and J. Toennies, Z. Phys. **214**, 472 (1968).
[7] R. David, M. Faubel, and J. Toennies, Chem. Phys. Lett. **18**, 87 (1973).
[8] G. Barg and J. Toennies, Chem. Phys. Lett. **51**, 23 (1977).
[9] G. Barg, G. Kendall, and J. Toennies, Chem. Phys. **16**, 243 (1976).

[10] A. A. Wu and F. O. Ellison, J. Chem. Phys. **47**, 1458 (1967).

[11] R. D. Poshusta, J. A. Haugen, and D. F. Zetik, J. Chem. Phys. **51**, 3343 (1969).

[12] J. Easterfield and J. W. Linnett, Nature (London) **226**, 142 (1970).

[13] R. C. Raffenetti and K. Ruedenberg, J. Chem. Phys. **59**, 5978 (1971).

[14] W. Kutzelnigg, V. Staemmler, and L. Hoheisel, Chem. Phys. **1**, 27 (1973).

[15] J. D. Switalski, J. T. J. Huang, and M. E. Schwartz, J. Chem. Phys. **60**, 2252 (1974).

[16] N. K. Ray and J. Switalski, Theor. Chim. Acta **41**, 329 (1976).

[17] N. K. Ray and S. P. Mehandru, Pramana **10**, 201 (1978).

[18] A. S. Zyubin, A. A. Gorbik, and O. P. Charkin, Zh. Strukt. Khim. **26**, 31 (1985).

[19] B. H. Cardelino, W. H. Eberhardt, and R. F. Borkman, J. Chem. Phys. **84**, 3230 (1986).

[20] D. A. Dixon, J. L. Gole, and A. Komornicki, J. Phys. Chem. **92**, 2134 (1988).

[21] D. A. Dixon, J. L. Gole, and A. Komornicki, J. Phys. Chem. **92**, 1378 (1988).

[22] L. A. Curtiss and J. A. Pople, J. Phys. Chem. **92**, 894 (1988).

[23] D. J. Searles and E. I. Von Nagy-Felsobuki, Phys. Rev. A **43**, 3365 (1991).

[24] B. K. Rao and P. Jena, Europhys. Lett. **20**, 307 (1992).

[25] I. Tamassy-Lentei and J. Szaniszlo, Acta Phys. Hung. **74**, 399 (1994).

[26] D. M. Bishop and S. M. Cybulski, Chem. Phys. Lett. **230**, 177 (1994).

[27] B. S. Jursic, Theor. Chim. Acta **491**, 11 (1999).

[28] R. Davy, E. Skoumbourdis, and T. Kompanchenko, Mol. Phys. **97**, 1263 (1999).

[29] E. Bodo, F. A. Gianturco, R. Martinazzo, A. Forni, M. Famulari, and A. Raimondi, J. Phys. Chem. A **104**, 11972 (2000).

[30] I. Tamassy-Lentei and J. Szaniszlo, THEOCHEM **501–502**, 403 (2000).

[31] M. Barbatti, G. Jalbert, and M. A. C. Nascimento, J. Chem. Phys. **114**, 2213 (2001).

[32] J. G. Vitillo, A. Damin, A. Zecchina, and G. Ricchiardi, J. Chem. Phys. **122**, 14311 (2005).

[33] I. Røeggen, H. Skullerud, T. Løvaas, and D. K. Dysthe, J. Phys. B **35**, 1707 (2002).

[34] V. P. Bulychev, K. M. Bulanin, and M. O. Bulanin, Opt. Spectrosc. **96**, 205 (2004).

[35] C. Sanz, E. Bodo, and F. A. Gianturco, Chem. Phys. **314**, 135 (2005).

[36] W. P. Kraemer and V. Špirko, Chem. Phys. **330**, 190 (2006).

[37] D. A. Wild and E. J. Bieske, Int. Rev. Phys. Chem. **22**, 129 (2003).

[38] C. Lovejoy, D. Nelson, and D. J. Nesbitt, J. Chem. Phys. **87**, 5621 (1987).

[39] D. A. Wild, P. S. Weiser, E. J. Bieske, and A. Zehnacker, J. Chem. Phys. **115**, 824 (2001).

[40] K. P. Huber and G. Herzberg, *Molecular Spectra and Molecular Structure IV. Constants of Diatomic Molecules* (van Nostrand Reinhold, New York, 1979).

[41] See EPAPS Document No. E-JCPSA6-126-003721 for line wave numbers and assignments. This document can be reached through a direct link in the online article's HTML reference section or via the EPAPS homepage (http://www.aip.org/pubservs/epaps.html).

[42] D. J. Nesbitt and R. Naaman, J. Chem. Phys. **91**, 3801 (1989).

[43] J. Tennyson, Comput. Phys. Rep. **4**, 1 (1986).

[44] U. Fink, T. Wiggins, and D. Rank, J. Mol. Spectrosc. **18**, 384 (1965).

[45] M. Okumura, L. Yeh, J. Myers, and Y. Lee, J. Phys. Chem. **94**, 3416 (1990).

[46] E. J. Bieske, S. A. Nizkorodov, F. R. Bennett, and J. P. Maier, J. Chem. Phys. **102**, 5152 (1995).

[47] L. Wolniewicz, J. Chem. Phys. **45**, 515 (1966).

[48] D. A. Wild, P. S. Weiser, and E. J. Bieske, J. Chem. Phys. **115**, 6394 (2001).

[49] D. A. Wild and E. J. Bieske, J. Chem. Phys. **121**, 12276 (2004).

[50] A. J. Page and E. I. von Nagy-Felsobuki, J. Phys. Chem. A **111**, 4478 (2007).